Wake potential and wake effects on the ionospheric plasma density measurements with sounding rockets

J. J. P. Paulsson[1], A Spicher[1], L. B. N. Clausen[1], J. I. Moen[1] and W. J. Miloch[1]

[1]Department of Physics, University of Oslo, Sem Sælands vei 24, Postbox 1048, 0317 Oslo, Norway

Key Points:

- Langmuir probe measurements
- Electric field measurements
- Wakes in plasma
- Object-plasma interaction

Corresponding author: J. J. P. Paulsson, j.j.p.paulsson@fys.uio.no

Abstract

A new method is developed to systematically study variations in the electrostatic potential around a spinning spacecraft in flowing plasma. We argue that the main modulation of this potential is due to wake leading to different depletions in electron and ion densities. This wake potential can be calculated with the help of electric currents measured by Langmuir probes mounted on a boom system and the assumption of Boltzmann distributed electrons. The wake position is determined with the electric field measurements. We apply this method to data from the ICI-3 ionospheric sounding rocket and find the observed wake to be larger than expected from the flow velocity and the Mach cone formation, which can be explained by the presence of booms. By using the wake potential to filter the rocket data, we show that this method is robust during highly dynamic plasma conditions, and that it can be used to improve the quality of plasma density measurements and reduce the wake effects.

1 Introduction

Instruments on-board sounding rockets can provide in-situ data for studying structures and processes of plasma in the ionosphere [*Kelley et al.*, 1982; *LaBelle et al.*, 1986; *Lorentzen et al.*, 2010; *Moen et al.*, 2012; *Spicher et al.*, 2016]. However, such in situ measurements can be influenced by the interactions between the rocket body and the surrounding plasma. The interactions can, as a consequence of electrical charging of the rocket, lead to the formation of an electrostatic sheath in the closest vicinity of the rocket body [*Whipple*, 1981]. Moreover, a plasma wake may form downstream of the rocket moving with respect to the plasma [*Al'pert et al.*, 1963; *Gurevich et al.*, 1969; *Liu*, 1969; *Samir et al.*, 1983; *Senbetu and Henley*, 1989; *Hutchinson*, 2012]. Wake disturbances can extend to large distances and their influences on data collection may occur even if the instruments are located far from the main rocket body. It is therefore important to properly account for the wake effects when analyzing data from sounding rocket experiments. Wake formation is a general problem concerning not only sounding rockets, but it also affects for example other types of spacecrafts [*Samir et al.*, 1979; *Miyake et al.*, 2013], and dusty plasmas [*Miloch et al.*, 2008; *Miloch*, 2014]. There is a limited in-situ data on the wake structures, which could allow to perform detailed qualitative and quantitative studies on such wakes. However, sounding rockets with instruments mounted on booms can provide unique pos-

sibility to characterize the wake structure [*Svenes et al.*, 1990; *Endo et al.*, 2015; *Darian et al.*, 2017].

For some spacecrafts, the payload instruments can be mounted in such a way that the measurements are minimally affected by the wake and the electrostatic sheath. However, for a spin stabilized rocket, the wake effects are difficult to avoid. For such rockets, the data can be modulated by the spin frequency of the rocket. An example are instruments mounted on booms, such as Langmuir probes, which allow for measurements of plasma density. Here, in data analysis, a commonly used method to account for wake modulations is a spectral band reject filter [*Jacobsen et al.*, 2010; *Spicher et al.*, 2015]. However, with this method, the modulations will be removed and the filtered data will be the average over the spin period. This is not physically justified since the wake in ionospheric conditions is characterized by a depletion in plasma density [*Al'pert et al.*, 1963; *Gurevich et al.*, 1969], and thus a proper filtering method should accurately remove the modulation without affecting the undisturbed (i.e., outside of wake) signal. It is therefore important to develop a new analysis method to estimate the wake potential and to account for the wake modulations of density measurements in a more physically sound manner.

In this paper we present a new method to study the wake potential and consequently account for wake modulations in the plasma density measurements with a spinning sounding rocket. We first calculate the electrostatic potential in the wake and then filter out the wake modulations from the measurements. We demonstrate that the new approach gives more accurate plasma density estimates as compared to a standard spectral band-reject filtering. To assess our method we use data provided by the Investigation of Cusp Irregularities 3 (ICI-3) [*Spicher et al.*, 2016] that has an array of cylindrical Langmuir probes mounted on booms at fixed biases which allow for a very high spatio-temporal resolution of the plasma density [*Bekkeng et al.*, 2010; *Jacobsen et al.*, 2010]. In section 2, we provide theoretical background on the wake formation in ionospheric plasmas. The outline of the method and short background on plasma density measurements is given in section 3. Section 4 presents the experimental setup of the ICI-3 rocket. We apply our method on ICI-3 data in section 5, discuss the results in section 6, and provide conclusions in section 7.

2 Wakes in ionospheric plasmas

In general when an object is placed in a flowing plasma, a wake will form downstream of the object, where the density of the plasma will be lower than the ambient plasma [*Al'pert et al.*, 1963; *Gurevich et al.*, 1969; *Liu*, 1969]. The density depletion in the wake is related to several properties of the plasma and of the object, such as the effective radius of the object R_0 scaled by the Debye length $R_D = R_0/\lambda_D$, the electron to ion temperature ratio $T = T_e/T_i$, the Mach number M, which is defined as the ratio between the drift velocity of the plasma v_D and the ion acoustic speed $C_S = \sqrt{k_B T_e/m_i}$, i.e., $M = v_D/C_S$, and the electric potential of the object scaled by the electron temperature $\Phi_r = e\phi_r/k_B T_e$ [*Al'pert et al.*, 1963; *Gurevich et al.*, 1969; *Liu*, 1969]. The quantities m_i, $e > 0$, and k_B correspond to the mass of ions, the elementary charge, and the Boltzmann's constant, respectively. Another important parameter is $R_M = MR_0$, since measurements in regions downstream of the object that are within R_M reveal apparent increase in electron temperatures [*Samir et al.*, 1986]. *Singh et al.* [1987] indicate that electron heating might occur in the closest vicinity of the objects body downstream, where only electrons with high velocity have access. Hence, R_M gives an approximate scale of the volume that flowing plasma has to fill. Due to wake dependence on multiple parameters, it is not straightforward to provide its detailed characterics.

2.1 Position of the wake

Another aspect is the position of the wake, which can be inferred from the direction of the plasma flow in the reference frame of the rocket [*Al'pert et al.*, 1963; *Gurevich et al.*, 1969; *Liu*, 1969]. In the ionosphere at high geomagnetic latitudes, the largest contribution to the plasma flow is the $\mathbf{E} \times \mathbf{B}$-drift [*Pécseli*, 2012]:

$$\mathbf{v}_{\mathrm{ExB}} = \frac{\mathbf{E} \times \mathbf{B}}{B^2}, \tag{1}$$

where $\mathbf{E}$, $\mathbf{B}$ are respectively electric and magnetic field vectors. A common method to determine the $\mathbf{v}_{\mathrm{ExB}}$ by sounding rockets is to measure the electric field [*Fahleson*, 1967; *Fahleson et al.*, 1970; *Mozer and Bruston*, 1967], which can then be combined with magnetic field according to Eq. 1. However, the electric field measured in the reference frame of the rocket includes also the electric field due to the rocket moving across the magnetic field lines. Thus, in the co-moving frame of the rocket, the plasma flow velocity must be determined from the vector relation $\mathbf{v}'_D = \mathbf{V} - \mathbf{v}_D$, where $\mathbf{V}$ is the velocity of the rocket

and $\mathbf{v}_D$ is the plasma flow velocity in the Earth-fixed frame, and $\mathbf{v}'_D$ is the plasma flow velocity in the co-moving frame. In the co-moving frame, the plasma flow velocity will be given by:

$$\bar{\mathbf{v}}'_D = \frac{\mathbf{E}' \times \mathbf{B}}{B^2}, \tag{2}$$

where $\bar{\mathbf{v}}'_D$ is the gyro-period averaged velocity, and $\mathbf{E}'$ refers to the electric field in a rocket co-moving reference frame.

At high geomagnetic latitudes, the magnetic field lines and the rocket body are approximately aligned and by assuming that the rocket motion is mainly perpendicular to the magnetic field lines which is often true for the central part of a rocket flight, Eq. (2) reduces to

$$\bar{v}'_D \approx \frac{E'}{B}, \tag{3}$$

and in this case velocity $\bar{\mathbf{v}}'_D$ will be perpendicular to the electric field. Note that both the electric field and drift velocity will be in the same plane that is perpendicular to the magnetic field [*Mozer and Bruston*, 1967]. The electric field measurements will also give the plasma flow direction in the rocket rest frame, as long as the main flow is perpendicular to the magnetic field lines. Thus, at high geomagnetic latitudes, configuration of the Earth's magnetic field allows for a good estimate of the plasma flow direction. Note however, that at low geomagnetic latitudes, the magnetic field might not be aligned with the rocket body and the plasma flow direction is not uniquely determined by the electric field measurements. For high-latitudes, a schematics of typical configuration of the spinning rocket, wake, plasma flow and electric and magnetic fields are presented in Figure 1. It shows that booms will enter the wake once per spin and that electric field measurements can be used for determining position of the wake, as it will be demonstrated in section 5.

2.2 Plasma density in the wake

The model of plasma inside the wake is important for a proper analysis of experimental results. In the ionosphere, sounding rockets tend to be much smaller than the mean free path of plasma particles, and a fluid model is most likely not suitable, and a kinetic model that includes interactions between the object and different plasma species is required [*Al'pert et al.*, 1963; *Gurevich et al.*, 1969; *Liu*, 1969]. Together with Maxwell's

equations a complete representation of the wake can in principle be found. In practice, this is not feasible and several simplifications have to be made. A complete discussion on such a model is beyond the scope of this article and the reader is referred to other works such as those by *Al'pert et al.* [1963]; *Gurevich et al.* [1969]; *Liu* [1969].

In the following, we give a description of the wake model that is relevant for our work, based on the articles above-mentioned: Assuming that $v_{te} >> v_D$, where v_{te} is the thermal velocity of electrons, we do not need to account for the drift velocity in the electron velocity distribution. This is a plausible assumption for sounding rockets in ionospheric plasmas, where the plasma flow is often close to the ion acoustic speed. Thus, the electron distribution in the wake can be approximated by the Maxwell-Boltzmann relation:

$$f_e(\mathbf{v}_e, \mathbf{r}) \simeq n_0 \left(\frac{m_e}{2\pi k_B T_e} \right)^{3/2} \exp\left(\frac{-m_e \mathbf{v}_e^2/2 + e\phi}{k_B T_e} \right), \tag{4}$$

where n_0 is the ambient plasma density, $\phi = \phi(\mathbf{r})$ is the electrostatic potential at position $\mathbf{r}$ in the rocket co-moving frame, $\mathbf{v}_e$ is the electron velocity, and m_e is the mass of the electrons. Eq. (4) is a solution to the Boltzmann equation in a conservative electrostatic force field [*Liboff*, 2003]. Note that Eq. (4) is only valid if all paths in phase-space are available, and hence at some distance away from the finite-sized object. As a consequence of the Maxwell-Boltzmann approximation the electron density n_e in the wake is given by:

$$n_e(\mathbf{r}) = n_0 \exp\left[\frac{e\phi(\mathbf{r})}{k_B T_e} \right]. \tag{5}$$

Thus, by taking that we are at a fair distance from the object surface, such that most of the paths in phase-space are available, and that the force field acting on the electrons is dominated by a conservative electrostatic force field, we can assume that electrons in the wake are Maxwell-Boltzmann distributed and their density is given by Eq. (5).

3 Determining the wake potential

Since the electron density depends on a local plasma potential, one needs to know the latter in order to assess in-situ plasma measurements. A common instrument for measuring plasma parameters in-situ is a Langmuir probe, which is often placed on a boom and enters the wake periodically [*Spicher et al.*, 2016]. We thus present how the Langmuir probe measurements can be utilised for determining a plasma potential in the wake.

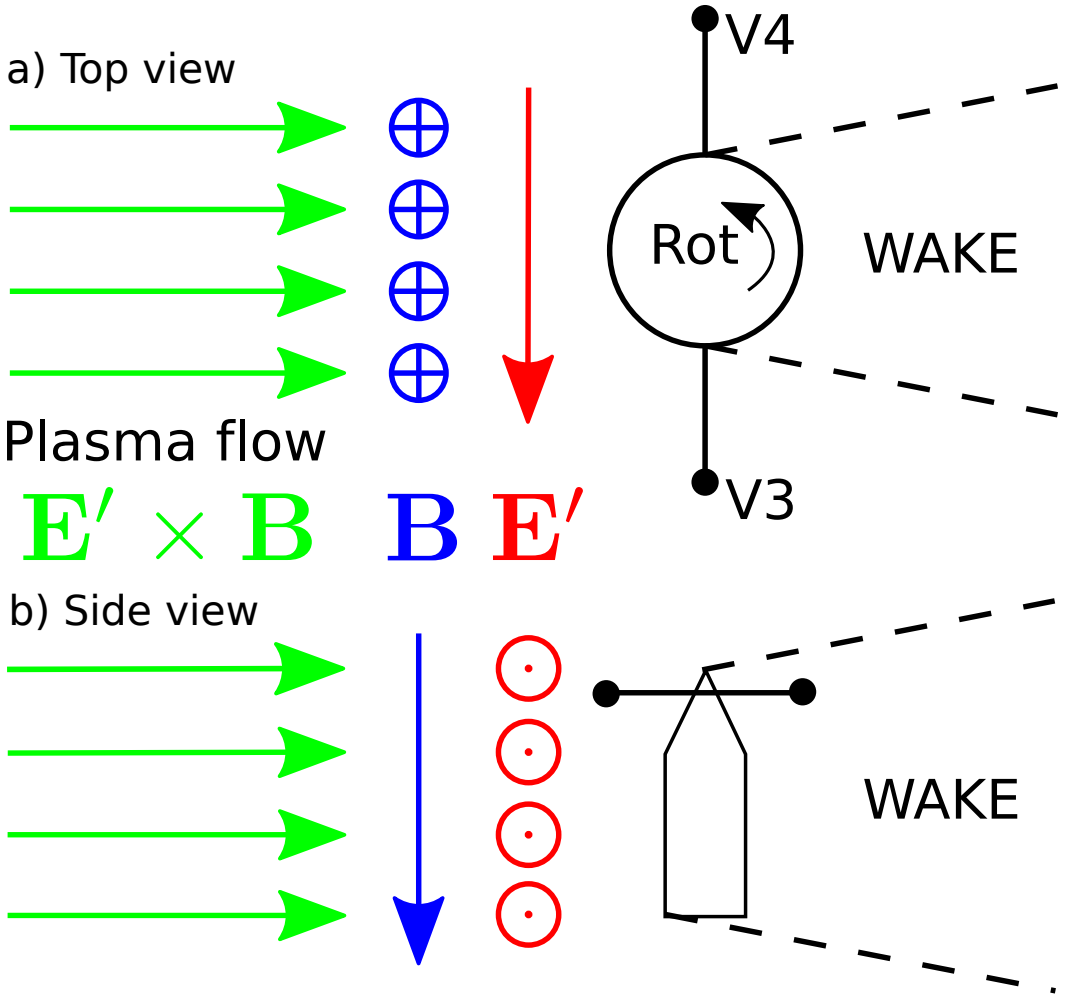

Figure 1. Schematics illustrating the orientation of the wake position with respect to boom-mounted probes on a rocket in an $\mathbf{E}' \times \mathbf{B}$-drifting plasma. The spin of the rocket (relevant for the ICI-3 rocket) is also indicated. $V4$ and $V3$ are the names of the probes, and will be defined and discussed in later sections.

3.1 Langmuir probe measurements

Langmuir probes collect electric currents from the surrounding plasma, and depending on the probe geometry and the velocity distribution of plasma, these currents can be related to plasma parameters. In the following, we will focus on cylindrical probes collecting only electrons, however similar reasoning can be extended to other probe probe geometries. Assuming that the velocity distribution of electrons is Maxwellian, the probe radius is much smaller than the Debye length in plasma, and that the bias potential voltage, V_b, of the probe satisfies:

$$V_b - V_p >> k_B T_e/e, \tag{6}$$

where V_p is the plasma potential, the current collected by a cylindrical probe with mantel area A_p, will be given by [*Mott-Smith and Langmuir*, 1926; *Schott*, 1968]:

$$I_{e0} = \frac{e n_e A_p}{4}\sqrt{\frac{8k_B T_e}{\pi m_e}}\frac{2}{\sqrt{\pi}}\sqrt{1+\frac{e(V_b-V_p)}{k_B T_e}}. \tag{7}$$

Note that, in general the total current to the probe can consist of currents due to plasma electrons and ions, photoemission, and secondary-emission. However, by having that Eq. (7) is the total current, we implicitly assume that the potential difference $V_b - V_p$ is large enough such that ion and photo-emission currents can be neglected. Due to relatively low energy of ions and electrons in the ionosphere, we also take that the emission of secondary electrons is negligible.

Eq. (7) shows that the current depends on the ratio: $e\left(V_b - V_p\right)/k_B T_e$. As discussed in section 2.2, the wake will have a depletion of electrons, due to a modified potential in the wake. In the wake, the current to the probe will depend on the ratio:

$$\frac{e\left(V_b - V_p + \phi(\mathbf{r})\right)}{k_B T_e}. \tag{8}$$

Thus, to calculate plasma parameters from Eq. (7) for the probe that is in the wake, it is essential to know $\phi(\mathbf{r})$, which gives the actual current to the probe.

$$I_e = \frac{e n_0 A_p}{4}\exp\left(\frac{e\phi}{k_b T_e}\right)\sqrt{\frac{8k_B T_e}{\pi m_e}}\frac{2}{\sqrt{\pi}}\sqrt{1+\frac{e(V_b-V_p+\phi(\mathbf{r}))}{k_B T_e}}. \tag{9}$$

Here, again, if the potential bias $V_b - V_p$ is large enough, we can assume

$$\frac{e\left(V_b - V_p + \phi(\mathbf{r})\right)}{k_B T_e} \simeq \frac{e\left(V_b - V_p\right)}{k_B T_e}, \tag{10}$$

and the largest effect of the wake on the current to the probe will be through a reduced electron density according to Eq. (5). This assumption is also supported by our results as

will be shown later. Hence, for a probe inside the wake, we have

$$I_e \simeq I_{e0} \exp\left[\frac{e\phi(\mathbf{r})}{k_B T_e}\right], \tag{11}$$

where I_{e0} is the electron current given by Eq. (7), which is undisturbed by the wake. By measuring the currents to the probe, the wake potential $\phi(\mathbf{r})$ at a given point can now be found by:

$$\frac{e\phi}{k_B T_e} = \ln\left(\frac{n_e}{n_0}\right) \simeq \ln\left(\frac{I_e}{I_{e0}}\right), \tag{12}$$

where for simplicity of notation, we have dropped the $\mathbf{r}$ dependence on the potential of the wake (as we will also do in the following).

3.2 Method to find the wake potential

The electron current measured by Langmuir probes mounted on booms can be combined with the electric field measurements to infer the potential of the wake of sounding rockets at high geomagnetic latitudes, provided that assumptions listed in the previous sections are valid. The wake potential can in turn be used to filter data and provide better estimates of the undisturbed plasma density, as compared to previously used methods.

Here, we present an overview of the method. We will explain the steps in more detail in the following sections, when applying the method to data collected by the ICI-3 sounding rocket. We assume that the density measuring instruments, which operate continuously in time with a fixed data-rate, periodically enter and exit the wake. The method for inferring the wake potential and filtering the data is characterized by the following steps:

1. Determine the direction of the plasma flow and find a region where the plasma is not perturbed by the wake. One way of doing this is to use the electric field measurements, as described in section 2.1.
2. Smooth data from the currents to the probe for density measurements (only required for measurements with high spatiotemporal resolution). This step will ensure that random spikes or dips measured in the unperturbed region as defined in step 1 will not significantly affect calculations of the potential in the wake. It will also ensure that small spatiotemporal fluctuations are not removed from the final result.
3. Record data points from the smoothed data (step 2) at the position of unperturbed plasma as defined in step 1. This will yield one data point from the current measurements each time the instrument is outside of the wake.

4. Interpolate between each data point collected according to step 3 to have an equal amount of samples as the raw data.
5. Apply Eq. (12) with n_0 (I_{e0} for Langmuir probes) being the raw density data, and n_e (I_e for Langmuir probes) being the baseline data as found through steps 1-4. This can be done sample-wise due to the interpolation in step 4.

4 Experimental Setup

To demonstrate the new method for extracting the potential of in the wake and assess its reliability, we use the plasma density measurements by the ICI-3 rocket. Investigation of Cusp Irregularities sounding rockets are a series of experiments designed to investigate cusp irregularities and their associated processes [*Lorentzen et al.*, 2010; *Moen et al.*, 2012; *Oksavik et al.*, 2012; *Moen et al.*, 2013].

4.1 The ICI-3 sounding rocket

The ICI-3 rocket was launched from SvalRak at Ny-Ålesund, Norway, at 07:21:31 UT on December 3, 2011. A sketch of the payload configuration showing the position of the different instruments as well as the rotation axis is presented in FIG. 2. The instruments used to derive the electron density and the DC electric field considered in this work were mounted on booms deployed perpendicular to the payload body. The booms were stored under a nose cone during launch and unfolded about 60 seconds into the flight. The electric field probes were mounted on the tips of the booms spanning 1740 mm, while the needle Langmuir probes were separated by about 1000 mm. For the DC electric field, using the potential difference between two sets of two probes separated in space by $\Delta x \simeq 1740$ mm we calculate $E'_{DC1} = -(V1 - V2)/\Delta x$ and $E'_{DC2} = -(V3 - V4)/\Delta x$ where $V1$, $V2$, $V3$ and $V4$ is the potential of probe 1,2,3 and 4 respectively (see FIG. 2 for more information), allowing to retrieve full electric field vector in the plane of the spin [*Fahleson*, 1967; *Fahleson et al.*, 1970; *Mozer and Bruston*, 1967]. Note that when the axis between the probes, for example for probes $V4$ and $V3$ as shown in FIG. 1, is parallel with the E'-field (see FIG. 1), E'_{DC2} will be a positive and should be the maximum for one rotation of the rocket. In the following, when we mention the E-field measured by DC2 we mean E'_{DC2}. For the electron density measurements, the instrument consists of 5 needle Langmuir probes with sampling rates of $f = 8680.5$ Hz [*Bekkeng et al.*, 2010; *Jacobsen et al.*, 2010]. They are referred to as NLP2, NLP4, NLP5, NLP6 and NLP8

(see FIG. 2), and had fixed bias voltages of 3.5 V, 3 V, 5 V, 4.5 V and 4 V with respect to the payload, respectively. For completeness, in FIG. 2, we also show other Langmuir probes that were mounted on the rocket payload: a spherical probe with fixed bias of 5 V mounted on the tip of the payload (*Sp*), as well as 3 spherical probes mounted on the booms (denoted s1, s3, and s7). The payload instruments also included sun sensors (not shown in the sketch), which can be used to determine the spin frequency and coning of the rocket.

4.2 The multi-needle Langmuir probe system

The multi-needle Langmuir probe system (m-NLP) is composed of very thin cylindrical probes, which are kept at different fixed bias voltages relative to the payload potential [*Bekkeng et al.*, 2010; *Jacobsen et al.*, 2010]. The radius of the cylinders is 0.255 mm, and the length is 25 mm. Since the cylinder radii are much less than the Debye length λ_D in the ionosphere, which is of the order of centimeters, and due to high thermal velocity of electrons as compared to the drift velocity of the plasma, Langmuir's orbital motion limited approximations modeling the currents, Eq. (7), received by the probe can be used [*Mott-Smith and Langmuir*, 1926; *Schott*, 1968].

An important observation of Eq. (7) is that the slope of I_e^2, with respect to V_b is independent on the electron temperature [*Jacobsen et al.*, 2010]. Furthermore, it is also independent of V_p. Due to these properties of I_e^2, one can determine the electron density independent of the electron temperature and of the floating potential of the rocket - which the probes are biased with respect to. Assuming that the electron temperature is equal in the vicinity of all the probes, one can then interpolate the slope of I_e^2 between the fixed biased needle-probes and obtain from Eq. (7):

$$n_e = \sqrt{\frac{\pi^2 m_e}{2e^3 A_p^3} \frac{d(I_e^2)}{dV_b}}. \tag{13}$$

It is evident that inaccuracies in calculating the electron density using this method may arise due to wake effects, since at each instances one probe can be in the wake but not the others. This can thus lead to different slopes of I_e^2 and, consequently, to erroneous values for n_e.

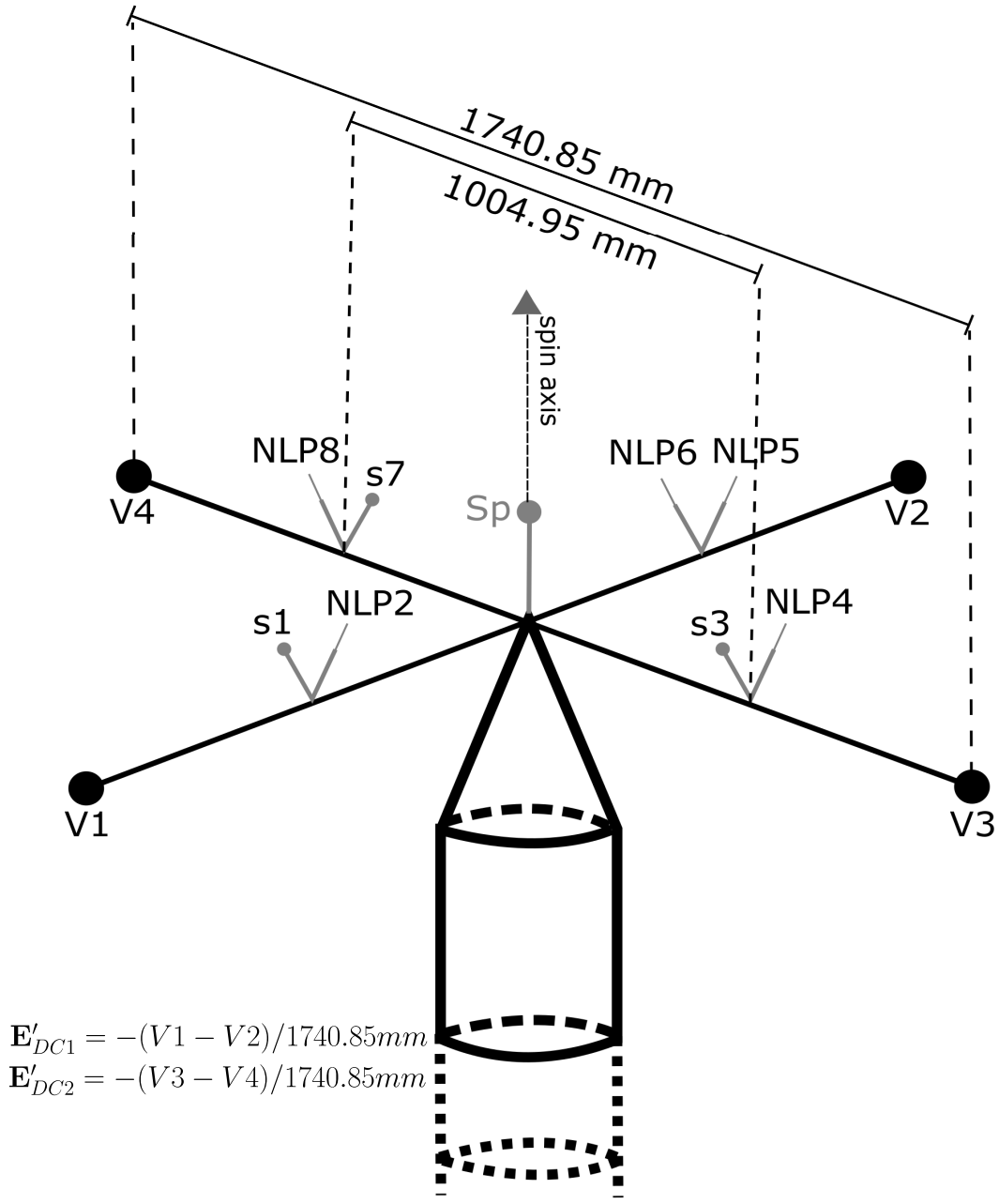

Figure 2. Schematics of the ICI-3 payload configuration: needle Langmuir probes (NLP), electric field probes (V1,V2,V3,V4) spherical probes (s1,s3,s7), and a fixed bias probe on the tip of the payload (Sp). Adapted from FIG. 1 in *Spicher et al.* [2016]

4.3 The wake around ICI-3

The plasma flow speed during the flight of ICI-3 ranged from subsonic to supersonic, depending on the mass of ions and plasma temperature considered. Due to a complicated geometry of the rocket, the effective radius R_0 is not straightforward to estimate. Since sizes of the rocket and the booms are macroscopic with respect to λ_D, it is expected that the wake created by the booms will have a non-negligible impact on the overall structure of the wake downstream of the rocket. Furthermore, one can attempt to estimate if the m-NLP's are located within the electron heating area R_M or not. The radius of the rocket body $R_0 \sim 0.2$ m can be taken as the determining length scale for the electron temperature enhancements in the wake. If we assume that $M \leq 2$ during most of the flight, then $R_M \leq 0.4$ m. Thus, the probes are outside R_M during most of the flight but might experience electron heating if the Mach number becomes excessively large. We assume that the electron temperature remains constant in the wake all the time during the flight since the Mach number seems to be $M \leq 2$ during the flight.

Expecting the depletion disturbance downstream of the rocket to expand with the ion acustic speed it is possible to estimate the resulting Mach cone where $\mu = \arcsin(1/M)$ is the half-angle of it. Using the estimated max $M = 2$ during the flight, we get $\mu = 30°$. This means that the probes on ICI-3 should only be experiencing the wake for 60° of a full rotation of the rocket, assuming that the wake is contained within the Mach cone related to the flow velocity.

The ICI-3 rocket body is made of a conducting metal and is being electrically charged by plasma currents. A good assumption is that all electrons are absorbed and ions are neutralized upon impact with the rocket [*Whipple*, 1981]. The neutral collision rate with plasma particles is very low at altitude above 150 km, and hence, in the vicinity of the rocket, neutrals do not interact with the plasma significantly. This means that we can neglect neutrals created by the ion impact on rocket body, and can assume that the rocket body acts as a perfect sink without compressing the plasma around the rocket. Furthermore, the m-NLP's are mounted at distances of several tens of λ_D from the body, i.e. we expect no sheath effects due to payload charging to be present in the measurements. Therefore, the plasma is close to be undisturbed outside of the wake. It is further assumed that the only significant disturbances of m-NLP's measurements are due to the wake effects.

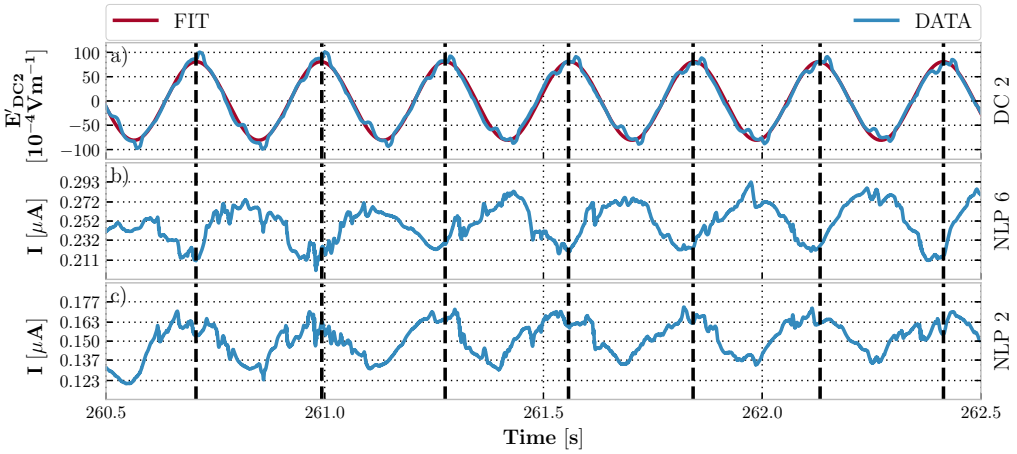

Figure 3. A sample of data from the ICI-3 rocket experiment, close to the middle of the flight. Thick dashed vertical lines correspond to when the E'_{DC2} double probe is aligned with the electric field. a) The electric field as measured by the probes V_4 and V_3 (blue) and a fit on the data with a sinusoidal function (red). b) The current collected by NLP6 that is in the wake when E'_{DC2} is positive. c) The current collected by NLP2 that is upstream when E'_{DC2} is positive.

5 Data analysis and results

5.1 Position of the wake

In section 2.1 we demonstrated that the wake position can be found by using the electric field measurements, which can provide the direction of the plasma flow in a co-moving frame. The convective electric field (E-field) vector is recovered from the double-probe system by noting that the E-field measurements will have a local minimum when the double-probe is parallel to the E-field vector. When the axis of the double-probe is perpendicular to the E-field vector, the potential difference between the probes is zero. When the axis is anti-parallel to the E-field vector, the potential difference has a local positive maximum, and so on. Hence, for one double-probe, during one rotation of the rocket, the E-field measurements will vary from a local maximum, go over to a zero value, then continue to a local minimum, and back again, as can be inferred from FIG. 1. It is therefore only possible to find the field strength and direction twice during a rotation. Thus, for one double-probe such as DC2, if we assume that the E-field does not vary much during the rotation, the E-field measurements can be well approximated by a sinusoidal function

[*Fahleson et al.*, 1970]. Accordingly, we fit a sinusoidal function to the E-field data around a peak for each spin of the rocket. This will reduce errors in finding the position of the local maximum or minimum.

Once the local extrema are identified, we find the plasma flow direction in the co-moving frame with Eq. (2) and by assuming that the magnetic field is parallel to the rocket body. Note that by adding another set of double-probes perpendicular to the first one, it is possible to obtain the full E-field vector at all times within the instruments sampling frequency capability. The set-up of ICI-3 allows for a full sampling of E-field, but this is not required for the purpose of our study, beacause we are here not concerned with variations of the wake at time scales at or below the rocket spin frequency.

A sample of data gathered during the ICI-3 experiment is presented in FIG. 3. FIG. 3a shows the E-field measurements from DC2 (blue) as well as a fit with a sinusoidal function (red). The fit shows that a sinusoidal function fits well to the measured E-field, and the direction of E-field is well marked for this particular experiment. Note that small uncertainties in the direction of E-field are not crucial for our method. FIG. 3b and FIG. 3c are the currents received by the NLP6 and NLP2 respectively. The wake can clearly be seen as a periodic decrease in the current collected. The vertical dashed lines correspond to the peaks of the electric field data found in the manner described above. One can see that the dashed lines do not coincide exactly with what is presumed to be the exact center of the wakes as represented by the NLPs. This small offset is most likely due to that the NPLs are slightly off-center of the booms. When the potential difference of DC2 has a local minimum, E-field will have a local maximum due to $\mathbf{E} = -\nabla\phi$. This means that when DC2 is negative (i.e., when $V4 - V3 < 0$), NLP6 will be in the wake downstream of the object and NLP2 will be directly upstream. This pattern is clearly visible in FIG. 3, as expected from the configuration presented in FIG. 2 and FIG. 1. The good agreement indicates that the instruments worked as expected during the flight, and thus data can be used for a further demonstration of the new method.

For the entire flight, the upstream position for every probe, which is spinning with the rocket, is found by either locating the maximum or minimum of the electric field measurements from DC1 and DC2, depending on the double-probe's position in relation to the NLP considered. This marks the upstream position where the density should be unaffected by the rocket motion, as indicated in section 2.

5.2 Calculation of the electrostatic potential in the wake

To calculate the potential of the wake, we use Eq. (12). I_{e0} is defined as the current received by the NLP at the upstream position, i.e. outside the wake, found by correlating the dataset with the E-field measurements. As an example, I_{e0} for each spin for NLP2 is found at time instances corresponding to the dashed vertical lines in FIG. 3. I_e of Eq. (12) is the current received during the following spin when the I_{e0} is found. However, two main questions arise at this point: i) where during the spin of the rocket does I_{e0}, which corresponds to one spin, go over to the value corresponding to the subsequent spin?; ii) and how much of the short-lived fluctuations are to be taken in the potential? The mNLP system provides measurements at a very high frequency, which allow for studying short-lived or small-scale structures [*Bekkeng et al.*, 2010; *Jacobsen et al.*, 2010], e.g. see FIG. 3. By simply employing Eq. 12 directly one would filter out all such structures, reducing the overall data quality.

We start by addressing the second issue: The potential is related to density fluctuations by the second derivative of the potential via Poisson's equation, and the second derivative tends to exaggerate fluctuations. It is thus natural for the potential to fluctuate less as compared to charge density. Thus, we smooth the currents I_e from individual NLP's with a moving window, using a normalized Gaussian window with a standard deviation of about 178.2 micro seconds, corresponding to 150 data points at the frequency of the m-NLP. This value has been chosen for pragmatic reasons: The time window needs to be shorter than the spin period of the rocket, but long enough to not allow the potential to contain all the short-lived fluctuations. Note that small structures in the resulting infered potential may be affected by using a different window, but as long as the magnitude of the wake in the currents to the probe are the same as the magnitude of the infered wake, in a relative sense, one can be sure that the overall structure of the infered potential corresponds to the measured data to a reasonable degree. Thus, fluctuations smaller than this window are not filtered from the raw currents. We will call the smoothed current I'_e.

As a solution to the first issue: We interpolate data using a cubic spline between I_{e0} for each spin to have the same sample size as I'_e. This minimizes fluctuations between the I_{e0}'s for each spin, but still allows for smooth transitions between I_{e0}'s in the subsequent spins. The interpolated I_{e0} will be called I'_{e0} in the following.

Since I'_e and I'_{e0} have the same sample frequency, we can now use Eq. (12) with sample wise division between I'_e and I'_{e0}. This means that $e\phi/k_BT_e$, which is obtained using Eq. (12), corresponds to the scaled potential around the rocket with I'_{0e} as reference point (meaning that $\phi = 0$ at this point). The results of the scaled potential calculations from two NLP's during a sample time of the flight are shown in FIG. 4. One can see that, for the most part, the wake potential is relatively consistent between the two probes, apart from some sporadic large-scale changes. Probes at different voltage bias, and thus collecting different currents, give the same wake pattern. Note that $e\phi/k_BT_e$ is the scaled potential around the rocket as measured by the NLPs, but we argue that most of the potential drop is due to the wake, and we will call $e\phi/k_BT_e$ the scaled wake potential, and accordingly ϕ the wake potential in the following.

FIG. 5 shows results for the entire flight of ICI-3. In FIG. 5a, for a visualization purpose only, we present a rough estimate of density calculated from the current to NLP2 by assuming an electron temperature of $T_e = 3000\ K$ and the payload potential of $-2\ V$. Note that the wake modulations are still present in the data in FIG. 5a. The scaled potential for NLP2 is presented in FIG. 5b. Finally, 5c shows the E-field measured by the double-probe DC2, while the altitude of the rocket is given in 5d. In FIG. 5 one can see that the wake potential does not vary much, even during large fluctuations in density or electric field, and in particular around the apogee of the flight, where the E-field measurements approximate the plasma flow direction the best.

As presented in section 2, the wake is characterized by the depletion in plasma density downstream of the rocket. The plasma will tend to fill this depletion, and since electrons have much higher thermal velocity than ions, the electrons will fill the depletion much deeper, with ions lagging behind. Thus, under stationary conditions, the wake should have a negative potential with respect to the ambient plasma. However, as it can be seen in FIG. 5 b) the wake potential is sometimes positive (corresponding mostly to upstream conditions). This is an effect of data processing: since electron plasma density fluctuates heavily, as can be seen in FIG. 3, the I_{e0} might in fact not be the local maximum current during that spin. This means that when finding the I_{e0} for one spin of the rocket, the current of the probe in question might be perturbed to a lower value than for currents before or after this point. This results in an inferred potential that is positive, and is indeed not part of the wake modulation. This should have already been potentially solved when we used I'_e to find the I_{e0}, but clearly this is not a complete remedy for this

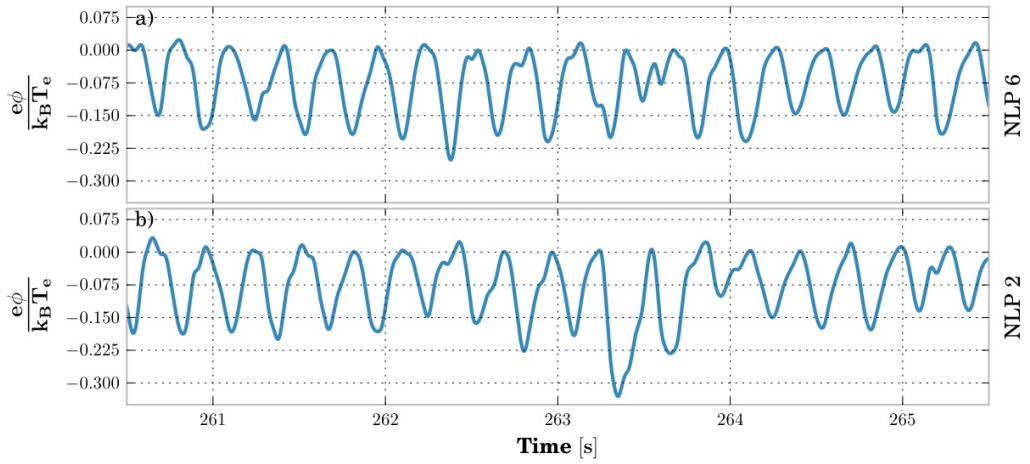

Figure 4. The scaled wake potential $e\phi/k_BT_e$ from a sample of data during the ICI-3 flight for a) NLP6 and b) NLP2.

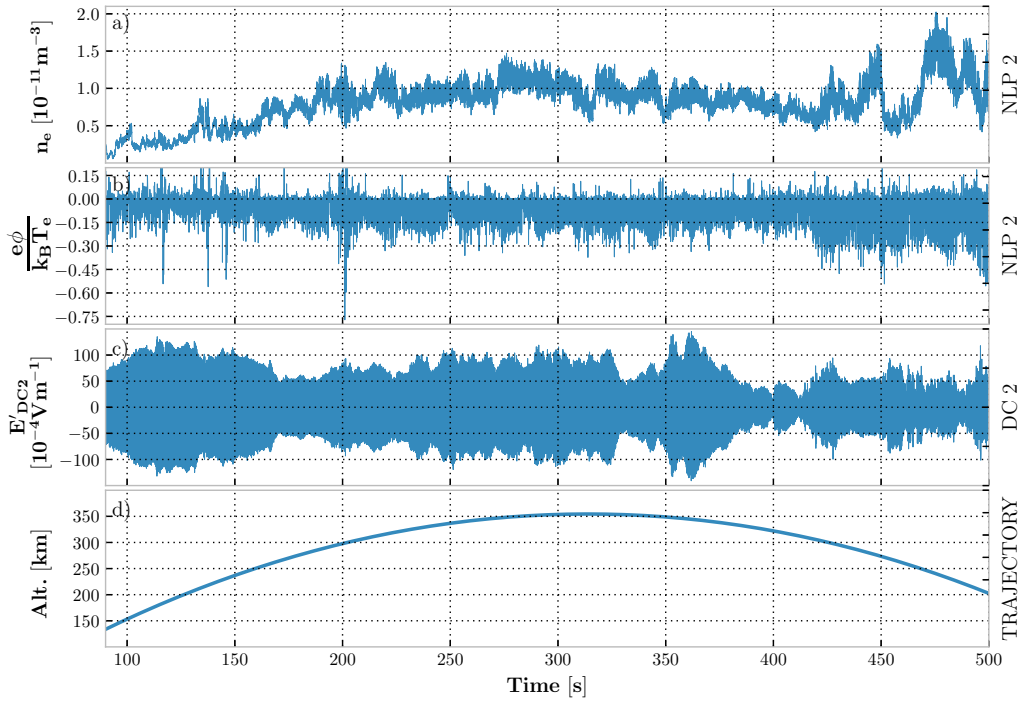

Figure 5. An overview of the whole flight of ICI-3: a) The electron density n_e calculated from NLP2 by assuming $T_e = 3000\ K$ and the payload potential of $-2\ V$. b) Scaled wake potential of the wake for NLP2. c) The electric field measured by the double-probe DC2. d) Altitude of the rocket as a function of time.

problem. An alternative approach would be to define edges of the wake (in a way similar to a Mach-cone) and take an average of currents that are outside of the wake. This is not straightforward since no clear edges are present in the data. Another way would be to take I_{e0} to be the maximum value that is sufficiently close to be directly upstream. However, both these alternative solutions seem artificial and do not have strong physical justification, in contrast to our method.

Note that in FIG. 5 b) the wake potential is more often positive before $t = 150$ s than for the rest of the flight. This may be attributed to the wake being less pronounced at that time because of a large vertical (i.e., parallel to **B**) velocity component of the rocket, and the plasma flow around the rocket not being coupled to the $\mathbf{E} \times \mathbf{B}$-drift only. With a large vertical velocity component upward, the wake shifts downwards along the rocket body. At around 200 s, large spikes are observed. These are due to large plasma fluctuations with time scales similar to, or shorter than the spin period of the rocket, making a systematic location of wake unreliable. After about 425 s, a more pronounced wake potential is observed, which may be attributed to a large vertical velocity of the rocket in the downward direction, and the wake shifting upwards along the rocket body. The rocket is also more tilted with respect to the flow direction during its down-leg, which further enhances the wake. In addition, the probes are mounted on top of the booms, thus being more likely in the wake on the downleg. Another clear signature seen in FIG. 5 is an enhancement of the wake with a regular period. This is due to a precession of the rocket during the flight.

5.3 Wake filtering and density estimates

With the wake potential established during the whole flight, we can now proceed to filtering of the NLP data for the wake effects. For this purpose, we combine Eq. (7) and Eq. (5), which results in Eq. (11). Then, by dividing both sides with the exponential function we obtain:

$$I_{wf} = I_e \exp\left[\frac{-e\phi}{k_B T_e}\right], \tag{14}$$

where I_e is the raw data from the NLPs, and the scaled wake potential $e\phi/k_B T_e$ is found by the routine described in the previous section. In the following, I_{wf} will be referred to as the wake filtered current. For comparison we also filtered out the wake modulation of the currents with a band-reject filter, as for instance done in *Jacobsen et al.* [2010] and

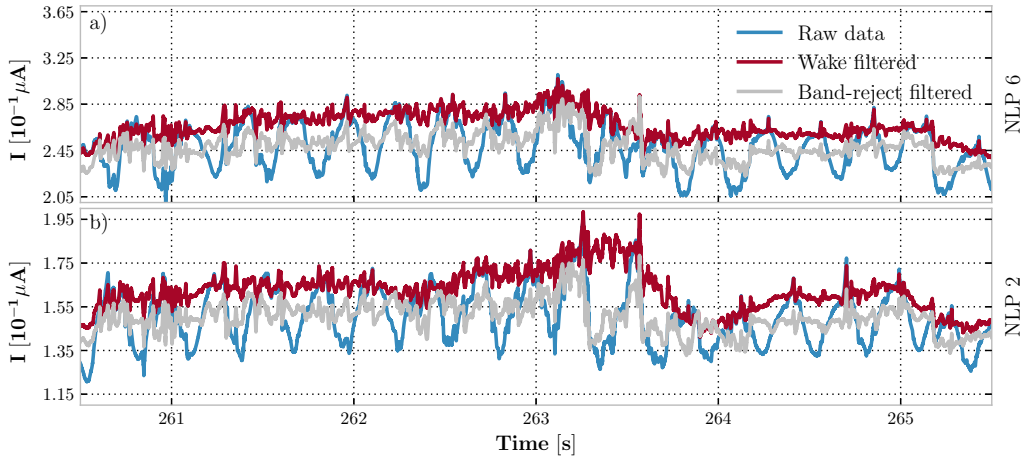

Figure 6. The raw current I_e (blue) collected by two NLPs on the ICI-3 rocket experiment, together with the wake filtered current I_{wf} (red) and band-reject filtered current I_{br} (gray) during a sample time interval of the ICI-3 flight. a) The data from NLP6. b) The data from NLP2.

we call this current I_{br}. The band-reject filter removes signals with frequencies close to the spin frequency of the rocket, as well as four harmonics of this frequency. The currents I_{wf} and I_{br}, together with the raw data I_e are shown in FIG. 6. As expected, the band-reject filter removes the wake modulations by replacing them with the approximate averages during the spin. In previous sections it was made clear that this is not physically sound to obtain an accurate value of the absolute electron density. Our new wake filtering technique reflects the undisturbed plasma to a higher degree. Not only it is closer to the conditions upstream compared to the band-reject filter, but it also handles the wake modulation much more effectively. A clear example of this can be seen in FIG. 6 b) around 263.5s. From the raw data one can see a strong wake modulation (see also the same period in FIG. 4 b)). The band-reject filter is not able to filter out this wake satisfactory, but our new wake filtering technique is successful.

The purpose of the m-NLP system is to measure the density reliably and independently of the electron temperature and of the payload charge. To illustrate this, we use NLP2, NLP5 and NLP6 to derive the density. NLP2 is located on a different boom than NLP5 and NLP6. It is therefore important to filter out the wake directly from the received current for each individual probe before calculating the density. As an illustrative comparison, we have also calculated the density from the raw data I_e. This can serve as a refer-

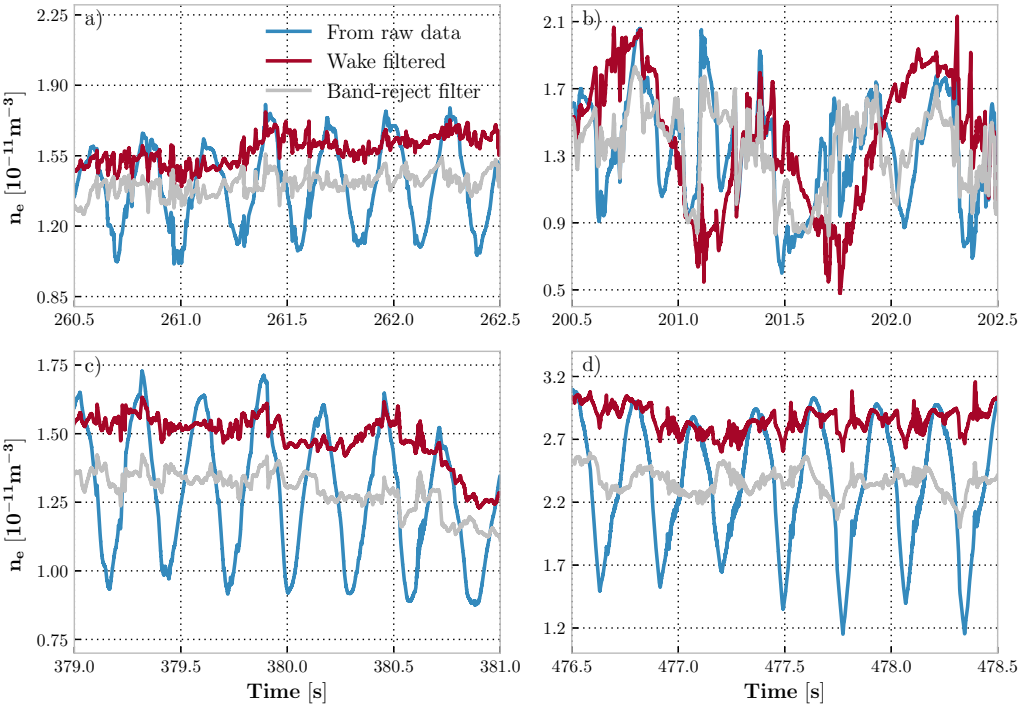

Figure 7. The derived electron plasma density n_e from the m-NLP system at intervals during the flight. Derived from the raw currents I_e (blue), from wake filtered currents I_{wf} (red), and from band-reject filtered currents I_{br} (gray). In panels a), c) and d) the wake filter is superior, while in panel b) both filtering techniques fail.

ence in comparison between the new wake filtering and the band-reject filtering methods, as it allows for estimating the relative effectiveness of the two filters.

In FIG. 7, a comparison between the two filtering techniques is presented, as well as the density derived from the raw data. Note that NLP5 and NLP6 will be in the wake simultaneously, since they were mounted on the same boom (see again FIG. 2). This means that the wake density depletion for the density derived from I_e gets enhanced, making the wake modulation more severe compared to the raw currents of individual probes. When NLP2 (located on the other side of the boom of NLP5 and NLP6) is in the wake, NLP5 and NLP6 are not, meaning that the slope of I_e^2 between different probes (see Eq. 13) becomes larger (since the bias voltage of NLP2 is the lowest of the three probes), which exaggerates the density slightly. Therefore, it is expected that the density derived from the filtered currents is close to the maximum density derived from the raw data during each spin. It should not, however, be exactly at the peak, since at these points NLP2 is in the wake, and as discussed above, the density is exaggerated slightly. This trend is exactly what we see in FIG. 7, panels a), c), and d).

In FIG. 7 b), however, both filtering techniques seem to fail. Recall, that in order to compensate for the wake effectivly, there must be a time period during the spin where it is possible to find a reliable reference point. If the plasma flutuates heavily such that a reference point is not easily found, the wake compensation method becomes unreliable. During the time period of FIG. 7 b), the plasma undergoes such large fluctuations at time scales shorter than the spin period of the rocket, and it becomes difficult to acertain a reliable reference point. When consulting the raw current to the probe, as well as the wake filtered currents, it is clear that both the location of the wake and the interpolation are not satisfactory in this particular event. When the plasma fluctuates with an amplitude larger than the wake modulation at time-scales shorter than the rocket spin period, assumptions for the method are no longer valid, and our new wake filtering method becomes unreliable.

6 Discussion

We have presented a new method to systematically infer the electrostatic potential around a sounding rocket from Langmuir probe current measurements. Modulations in this potential are dominated by the depletion of plasma in the wake, and hence we call this potential the wake potential. The main goals are the following: i) To provide new

possibilities to study wake structures in more detail around objects with complex geometry, ii) and to improve the quality of the plasma measurements in cases where wakes cannot be avoided. Our new method can successfully and in a systematic way, infer the wake potential around a spinning object with arbitrary geometry. It can therefore provide valuable data on the wake structure for a variety of plasma parameters. By being applied to Langmuir probe measurements on the ICI-3 sounding rocket, the approach has also proven to be successful in improving the quality of measurements that have been affected by wakes.

The electrostatic potential of a wake is a complex phenomenon, and its dependence on local plasma conditions is non-trivial. However, some features of the wake are expected for ionospheric sounding rockets: The electrons should be Boltzmann distributed in the wake at distances far away form the object, the plasma should be undisturbed outside of the wake with no shock present (i.e., no build-up of plasma density upstream), and the wake disturbance will expand downstream of the object [*Al'pert et al.*, 1963; *Gurevich et al.*, 1969; *Liu*, 1969]. The electrons are Boltzmann distributed as long as the plasma flow velocity is small compared to the thermal velocity of the electrons [*Liboff*, 2003], and at distances from the object so that most of the trajectories in phase-space can be populated. This is justified for the ICI-3 sounding rocket: at a distance of the probe in the wake R_p, only electrons with velocity such that $R_0/v_e < R_p/\bar{v}'_D$ have time to reach the probe. Since R_0 and R_p for ICI-3 are comparable and $v_{te} \gg \bar{v}'_D$ in the ionosphere, most of the electrons can reach the probe, and the distribution of electrons is close to Boltzmann.

Furthermore, in most cases it is appropriate to consider a conductive object in the ionosphere to be a perfect sink of charges [*Whipple*, 1981]. That is, all electrons impacting the object will be absorbed, and all ions will be neutralized by the impact. The resulting neutrals will not interact with the plasma in any significant amount close to the object [*Al'pert et al.*, 1963]. Hence, there will be no build-up region of plasma around the object. For ICI-3, the potential measurements around the rocket should then always be below zero. However, in FIG. 4 and 5 one can see that the wake potential is sometimes above zero, which is due to the analysis method. In FIG. 3 one can see that the current to the probes fluctuates significantly upstream of the rocket. This leads to I_{e0} that can be lower than the maximum around the upstream point, even though it is found from the smoothed current I'_e. This does not have any significant effect on the quality of the calculated wake

potential data, and one should however not interpret these as a plasma build-up region without carefully consulting the raw currents from the Langmuir probes.

Another feature of the wake potential is that the wake disturbance downstream of the object should propagate to the undisturbed regions perpendicular to the flow directions at the speed of the ion acoustic speed. However, as can be seen in FIG. 4 the probes seem to be in the wake during a majority of the spins, i.e., the wake seems to be large enough to include the probes such they are affected by it for a majority of the rocket rotation. As we mentioned earlier, if the wake could be completely characterised by a Mach cone, the probes should be in the wake for approxmatly 60° of the full rotation, as also shown in simulations [*Darian et al.*, 2017]. The most obvious contributor to this effect are the booms, but it is also worth mentioning that the wake might not be fully characterised by a Mach cone. *Miyake et al.* [2013] showed that booms can significantly enlarge the wake. Furthermore, the 3-D structure of the wake can contribute to this as well. Referring to FIG. 5, during the up- and down-leg of the flight, there might have been a significant plasma flow parallel to the spin vector of the rocket. This can lead to unpredictable structure of the wake due to the complex geometry of the rocket. Another intricacy in the signal can be attributed to the precession of the rocket, which introduces a low frequency modulation in the data. Note that our new method is invariant to the exact geometry of the object that creates the wake. As long as there is one point during the spin that corresponds to undisturbed plasma condition, the method will work by using that point as a reference.

We demonstrate that the wake potential can be used to improve the quality of density measurements that are affected by the wake depletion. This is for example important for studies relying on accurate plasma density measurments, for deriving the absolute plasma densities, characterisation of plasma fluctuations, plasma irregularities and turbulence. In FIG. 6 we apply the method to the electron currents collected by the NLPs during the sounding rocket flight, and compare to results obtained with a standard spectral band-reject filter. The wake filtering method appears to be much closer to the undisturbed plasma during the spins of the rocket, whereas the band-reject method gives the average between the current from the density depleted regions due to the wake and the undisturbed density. We argue in sections 2 and 4.3 that there should not be a region of enhanced plasma density around the rocket. The wake filtering method is also more efficient than the band-reject filter in filtering out all of the wake modulations, as can be seen in FIG. 6

b) around 263.5s, where the band-reject filter fails but the wake filter works nominally. Hence, the wake filtering method is more physically sound as compared to the spectral band-reject method, and can improve the quality of density measurements. FIG. 7 shows that the band-reject filter underestimates the density, as much as around 20%, and that the wake filtering method indeed gives a much improved data.

The method that we have introduced has some limitations. First, it is restricted to high geomagnetic latitudes as the main part of the plasma flow has to be related to the $\mathbf{E} \times \mathbf{B}$-drift in order to use the E-field measurements. However, note that it would also be possible to use the signature of the wake itself to locate the direction of the wake, and hence our method could also be applied to other situations. One has to be careful though, since some studies have found that the presence of the magnetic field can lead to asymmetries in the wake [*Grabowski and Fischer*, 1975; *Darian et al.*, 2017]. It is also important to choose a proper smoothing function, which will account for the physical phenomena of interest. Finally, the very dynamic plasma conditions at time scales shorter than the spin of the rocket can be challenging, as indicated in FIG. 7b. The method works well as long as variations in the background plasma density are at time scales longer than the spin. This is the case for most of the ICI-3 flight, which was indeed through a very dynamic plasma conditions including a reverse flow event [*Rinne et al.*, 2007]. Details on these plasma conditions can be found in *Spicher et al.* [2016].

One striking result is the wake does not exhibit large variations, as can be seen in FIG. 5b. Comparing with the fluctuations of E-field in FIG. 5c one can see that the strength of the wake seems not to be strongly correlated with the flow of the plasma. Certainly, there are more plasma parameters than just E-field strength, which will affect the structure and strength of the wake potential, and this is an a subject of future studies. A possible explanation for the stability of the wake can be that, according to *Al'pert et al.* [1963] the probes are close enough to the body so that the wake potential is dominated by the floating potential of the body. This would then suggest that the floating potential of the body does not vary much, implying that the plasma temperature and the particle precipitation do not vary much during most of the flight. The large enhancement of the wake after 425s can then be explained by an increase in particle precipitation which would make the floating potential significantly more negative. *Spicher et al.* [2016] reports an increase of particle precipitation energy and energy flux around this time, which makes this a plausible scenario. However, this is a topic for further investigation.

Another topic for further investigation is how much the strength and the structure of the wake are affected by the booms. A more complete picture of the wake phenomena in the ionosphere, can be obtained by including more plasma parameters, such as ion composition and electron temperature. To improve the quality of this method, one could also include a model on how the magnetic field alters the distribution of electrons in the wake, as well as shielding of trajectories of electrons by the object. Nevertheless, with this new method, one can already now significantly improve the reliability of density measurements, as well as our understanding on optimal instrument placements on board of spinning spacecrafts.

7 Summary

We have developed a new method to systematically infer the potential around an object in a flowing plasma from density measurements. We argue that the main modulation of this potential is the plasma wake that creates a difference in density depletion between the electrons and ions. We call this potential the wake potential. We have shown that it is possible to correlate the electric field measurements to the wake position, and with this calculate the wake potential assuming Boltzmann distributed electrons. Using density measurements from the ICI-3 sounding rocket to asses this method, we found that the wake seems to be significantly large, which might be explained by the presence of the booms. The wake potential is also affected by the 3-D structure of the wake. Furthermore, we show that this method is robust during a highly dynamic plasma conditions, and can be used to improve the quality of density measurements that are affected by the wake.

Acknowledgments

The authors would like to thank T. A. Bekkeng and E. Trondsen for support on and for providing the data for ICI-3. We also wish to thank A. Pedersen for discussions, especially regarding the electric field measurements. This study is supported in part by the Research Council of Norway grant no. 208006, 230996, and 240000. Payload services, rocket hardware and launch operations were funded through the Norwegian Space Center and delivered by Andøya Space Center. This study is a part of the 4DSpace initiative. The data used in this study is provided by *Paulsson* [2018]. The authors thank the reviewers for constructive comments.

References

Al'pert, Y. L., A. V. Gurevich, and L. P. Pitaevskiĭ (1963), Effects produced by an artificial satellite rapicly moving in the ionsophere or in an interplanetary medium, *Sov. Phys. Usp.*, *6*(1), 13, doi:10.1070/PU1963v006n01ABEH003492.

Bekkeng, T. A., K. S. Jacobsen, J. K. Bekkeng, A. Pedersen, T. Lindem, J.-P. Lebreton, and J. I. Moen (2010), Design of a multi-needle Langmuir probe system, *Meas. Sci. Technol.*, *21*(8), 085,903, doi:10.1088/0957-0233/21/8/085903.

Darian, D., S. Marholm, J. J. P. Paulsson, Y. Miyake, H. Usui, M. Mortensen, and W. J. Miloch (2017), Numerical simulations of a sounding rocket in ionospheric plasma: Effects of magnetic field on the wake formation and rocket potential, *Journal of Geophysical Research: Space Physics*, *122*(9), 9603–9621, doi:10.1002/2017JA024284, 2017JA024284.

Endo, K., A. Kumamoto, and Y. Katoh (2015), Observation of wake-induced plasma waves around an ionospheric sounding rocket, *J. Geophys. Res. Space Physics*, *120*(6), 2014JA020,047, doi:10.1002/2014JA020047.

Fahleson, U. (1967), Theory of electric field measurements conducted in the magnetosphere with electric probes, *Space Science Reviews*, *7*(2-3), 238–262.

Fahleson, U. V., M. C. Kelley, and F. S. Mozer (1970), Investigation of the operation of a d.c. electric field detector, *Planetary and Space Science*, *18*(11), 1551–1561, doi:10.1016/0032-0633(70)90030-9.

Grabowski, R., and T. Fischer (1975), Theoretical density distribution of plasma streaming around a cylinder, *Planetary and Space Science*, *23*(2), 287–304.

Gurevich, A. V., L. P. Pitaevskii, and V. V. Smirnova (1969), Ionospheric aerodynamics, *Space Science Reviews*, *9*(6), 805–871.

Hutchinson, I. H. (2012), Electron velocity distribution instability in magnetized plasma wakes and artificial electron mass, *Journal of Geophysical Research: Space Physics*, *117*(A3), doi:10.1029/2011JA017119.

Jacobsen, K. S., A. Pedersen, J. I. Moen, and T. A. Bekkeng (2010), A new Langmuir probe concept for rapid sampling of space plasma electron density, *Meas. Sci. Technol.*, *21*(8), 085,902, doi:10.1088/0957-0233/21/8/085902.

Kelley, M. C., R. Pfaff, K. D. Baker, J. C. Ulwick, R. Livingston, C. Rino, and R. Tsunoda (1982), Simultaneous rocket probe and radar measurements of equatorial spread fâĂŤtransitional and short wavelength results, *Journal of Geophysical Research: Space*

Physics, *87*(A3), 1575–1588, doi:10.1029/JA087iA03p01575.

LaBelle, J., M. C. Kelley, and C. E. Seyler (1986), An analysis of the role of drift waves in equatorial spread f, *Journal of Geophysical Research: Space Physics*, *91*(A5), 5513–5525, doi:10.1029/JA091iA05p05513.

Liboff, R. L. (2003), *Kinetic Theory: Classical, Quantum, and Relativistic Descriptions*, Springer Science & Business Media.

Liu, V. C. (1969), Ionospheric gas dynamics of satellites and diagnostic probes, *Space Sci Rev*, *9*(4), 423–490, doi:10.1007/BF00212707.

Lorentzen, D. A., J. Moen, K. Oksavik, F. Sigernes, Y. Saito, and M. G. Johnsen (2010), In situ measurement of a newly created polar cap patch, *J. Geophys. Res.*, *115*(A12), A12,323, doi:10.1029/2010JA015710.

Miloch, W. J. (2014), Numerical simulations of dust charging and wakefield effects, *Journal of Plasma Physics*, *80*(6), 795–801, doi:10.1017/S0022377814000300.

Miloch, W. J., J. Trulsen, and H. L. PÃľcseli (2008), Numerical studies of ion focusing behind macroscopic obstacles in a supersonic plasma flow, *Phys. Rev. E*, *77*(5), 056,408, doi:10.1103/PhysRevE.77.056408.

Miyake, Y., C. M. Cully, H. Usui, and H. Nakashima (2013), Plasma particle simulations of wake formation behind a spacecraft with thin wire booms, *Journal of Geophysical Research: Space Physics*, *118*(9), 5681–5694, doi:10.1002/jgra.50543.

Moen, J., K. Oksavik, T. Abe, M. Lester, Y. Saito, T. A. Bekkeng, and K. S. Jacobsen (2012), First in-situ measurements of HF radar echoing targets, *Geophys. Res. Lett.*, *39*(7), L07,104, doi:10.1029/2012GL051407.

Moen, J., K. Oksavik, L. Alfonsi, Y. Daabakk, V. Romano, and L. Spogli (2013), Space weather challenges of the polar cap ionosphere, *Journal of Space Weather and Space Climate*, *3*(27), A02, doi:10.1051/swsc/2013025.

Mott-Smith, H. M., and I. Langmuir (1926), The Theory of Collectors in Gaseous Discharges, *Phys. Rev.*, *28*(4), 727–763, doi:10.1103/PhysRev.28.727.

Mozer, F. S., and P. Bruston (1967), Electric field measurements in the auroral ionosphere, *J. Geophys. Res.*, *72*(3), 1109–1114, doi:10.1029/JZ072i003p01109.

Oksavik, K., J. Moen, M. Lester, T. A. Bekkeng, and J. K. Bekkeng (2012), In situ measurements of plasma irregularity growth in the cusp ionosphere, *Journal of Geophysical Research: Space Physics*, *117*(A11), n/a–n/a, doi:10.1029/2012JA017835, a11301.

Paulsson, J. J. P. (2018), Ici3 derived wake potential and density data, doi: 10.5281/zenodo.1194905.

Pécseli, H. L. (2012), *Waves and Oscillations in Plasmas*, CRC Press.

Rinne, Y., J. Moen, K. Oksavik, and H. C. Carlson (2007), Reversed flow events in the winter cusp ionosphere observed by the european incoherent scatter (eiscat) svalbard radar, *Journal of Geophysical Research: Space Physics*, *112*(A10), n/a–n/a, doi: 10.1029/2007JA012366, a10313.

Samir, U., R. Gordon, L. Brace, and R. Theis (1979), The near-wake structure of the Atmosphere Explorer C (AE-C) Satellite: A parametric investigation, *J. Geophys. Res*, *84*(A2), 513–525, doi:10.1029/JA084iA02p00513.

Samir, U., K. H. Wright, and N. H. Stone (1983), The expansion of a plasma into a vacuum: Basic phenomena and processes and applications to space plasma physics, *Rev. Geophys.*, *21*(7), 1631–1646, doi:10.1029/RG021i007p01631.

Samir, U., N. H. Stone, and K. H. Wright (1986), On plasma disturbances caused by the motion of the space shuttle and small satellites: A comparison of in situ observations, *J. Geophys. Res.*, *91*(A1), 277–285, doi:10.1029/JA091iA01p00277.

Schott, L. (1968), Electrical probes, *Plasma diagnostics*, pp. 668–731.

Senbetu, L., and J. R. Henley (1989), Distribution of plasma density and potential around a mesothermal ionospheric object, *Journal of Geophysical Research: Space Physics*, *94*(A5), 5441–5448, doi:10.1029/JA094iA05p05441.

Singh, N., U. Samir, K. H. Wright, and N. H. Stone (1987), A possible explanation of the electron temperature enhancement in the wake of a satellite, *J. Geophys. Res.*, *92*(A6), 6100–6106, doi:10.1029/JA092iA06p06100.

Spicher, A., W. J. Miloch, L. B. N. Clausen, and J. I. Moen (2015), Plasma turbulence and coherent structures in the polar cap observed by the ici-ï£¡2 sounding rocket, *Journal of Geophysical Research: Space Physics*, *120*(12), 10,959–10,978, doi: 10.1002/2015JA021634.

Spicher, A., A. A. Ilyasov, W. J. Miloch, A. A. Chernyshov, L. B. N. Clausen, J. I. Moen, T. Abe, and Y. Saito (2016), Reverse flow events and small-scale effects in the cusp ionosphere, *J. Geophys. Res. Space Physics*, *121*(10), 2016JA022,999, doi: 10.1002/2016JA022999.

Svenes, K. R., J. Trøim, B. N. Maehlum, M. Friedrich, K. M. Torkar, G. Holmgren, and W. F. Denig (1990), Ram-wake measurements obtained from the ionospheric sound-

ing rocket MAIMIK, *Planetary and Space Science*, *38*(5), 653–663, doi:10.1016/0032-0633(90)90072-X.

Whipple, E. C. (1981), Potentials of surfaces in space, *Rep. Prog. Phys.*, *44*(11), 1197, doi:10.1088/0034-4885/44/11/002.